The Satellite Ferrimagnetic Power Limiter

By L. J. VARNERIN, R. L. COMSTOCK,
W. A. DEAN and R. W. KORDOS

(Manuscript received February 11, 1963)

To limit the 4080-mc local oscillator signal power input to the beat oscillator modulator of the Telstar satellite communications repeater, a subsidiary absorption limiter was used which consisted of an optically polished sphere of single-crystal yttrium iron garnet (YIG), placed in a resonant transmission cavity between the amplified 4080-mc output of the traveling-wave tube and the BO modulator input. The limiter holds the output power nearly constant above a given input threshold; below this threshold the YIG is linear and introduces only a small loss. The threshold is determined, for a given sample at a given frequency, by the external magnetic bias field. Temperature compensation over the desired range was obtained by orienting the crystal with the dc magnetic field along a [100] or "hard" axis. The total weight of the limiter package, including the bias magnet and cavity, is 13 ounces.

I. INTRODUCTION

The traveling-wave tube[1] in the Telstar communications repeater[2] serves to amplify both the 4170-mc output signal and the low-level (−12 dbm) 4080-mc local oscillator-beacon signal. The TWT gain for the 4080-mc signal is strongly dependent upon the 4170-mc signal level. If the signal to the satellite is lost, no 4170-mc signal is generated and the gain for the 4080-mc signal increases significantly. Additionally, temperature variations can cause undesired level changes. As can be seen from Fig. 1 of Ref. 2, the 4080-mc signal is the local oscillator for the beat oscillator modulator, which generates the 6300-mc local oscillator signal for the input down converter. This increased 4080-mc level can cause the modulator to oscillate.

To eliminate these effects a microwave ferrimagnetic power limiter was designed and incorporated to limit the 4080-mc level. Because this type of limiter incorporates a resonant cavity, it serves a required filter func-

tion of rejecting undesired signals which might cause instability. The limiter cavity loaded Q was designed to fulfill this need.

1.1 *Properties of Limiters*

Microwave power limiters are passive two-port devices which limit output power to a nearly constant value beyond some input threshold power level. Below this threshold limiters are linear and ideally introduce negligible loss. At a single frequency the power output (P_o) vs available power input (P_a) response of a limiter is shown in Fig. 1. The two thresholds, $P_{o\ crit}$ and $P_{a\ crit}$, are indicated as well as the shape of the limiting characteristic below and above the threshold. In the Telstar satellite application the limiter electrical and mechanical requirements are given in Table I and the mechanical requirements will be discussed in Section III. The temperature behavior of the device will be considered in detail in Section II.

Degenerate parametric oscillators make possible excellent power limiting devices, in which case the signal to be limited is used as the "pump" signal. Above the oscillation threshold the losses in the pump circuit increase since energy is required to sustain the oscillation, resulting in power limiting. For microwave ferrimagnets the pump circuit is the uniform precession motion of the magnetization coupled to a microwave circuit, and the parametrically excited systems are the "spin waves" which are bounded by the sample and not coupled to the external circuitry. A ferrimagnetic limiter employing single-crystal yttrium iron garnet (YIG) was chosen for the satellite requirements.

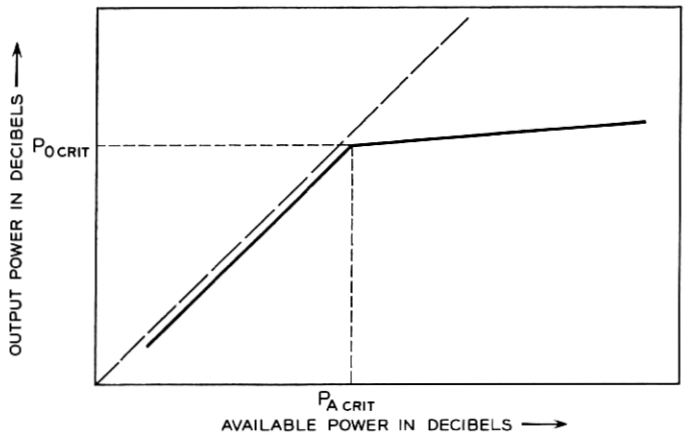

Fig. 1 — Output power (P_o) vs available power (P_a) for a power limiter.

TABLE I — POWER LIMITER REQUIREMENTS

Frequency of operation: 4080 mc
Bandwidth: to have a loaded Q of about 200
Quiescent point of operation: +14.5 dbm output power at +18.0 dbm input power
Output power at +26.0 dbm input power: < +17 dbm
Insertion loss below limiting level: <1.0 db
Temperature range of operation: +35°F to +120°F
Waveguide: silver-plated magnesium.

1.2 *The Subsidiary Absorption*

The degenerate parametric coupling of half-frequency spin waves in a ferrimagnet by the uniform precession has been discussed by Suhl.[3] Suhl's theory gives the threshold RF magnetic field at the sample (h_{crit}) as a function of the dc bias magnetic field, as shown in Fig. 2 for spherical samples. The ordinate is the ratio of h_{crit} to ΔH_k, the "spin wave" linewidth, while the abcissa is the ratio of the precession frequency, $\omega_o = \gamma H_e$ to the operating frequency ω, where γ is the gyromagnetic ratio. H_e is an effective bias field, the sum of the bias magnetic field H_{dc} and H_a the anisotropy field appropriate to the crystallographic axis with which H_{dc} coincides (see Section II). ω_m is $\gamma 4\pi M_s$, where $4\pi M_s$ (1750 oersteds for

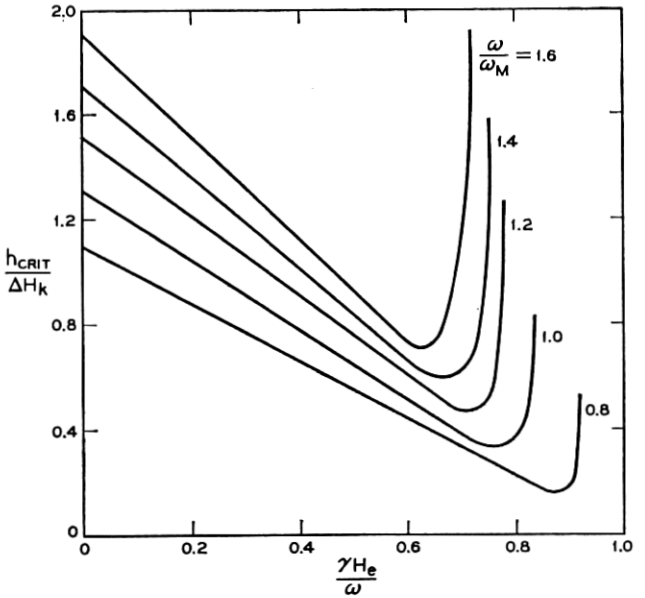

Fig. 2 — The subsidiary absorption threshold (h_{crit}) vs $\gamma H_e/\omega$ with ω/ω_M as a parameter (from Ref. 3).

YIG) is the ferrimagnetic saturation magnetization. The subsidiary absorption described by this curve always occurs at field values less than the resonance value, $(\omega_o/\omega) = 1$. For 4-kmc operation with YIG, ω/ω_M is 0.816. It is apparent from these curves that the threshold for the subsidiary absorption can be varied at a given frequency by varying the magnetic bias field. Above the threshold for the subsidiary absorption the losses in the ferrite sample increase, resulting in power limiting.

1.3 *The Ferrimagnetic Limiter*

A photograph of the completed limiter with the biasing magnet in position is shown as Fig. 3. A single-crystal spherical sample of YIG was mounted in the transmission resonant cavity and biased to the subsidiary absorption, with the external dc magnetic field perpendicular to the RF magnetic fields of the cavity mode. Single-crystal YIG was used since in this material the spin wave linewidth ΔH_k is extremely low

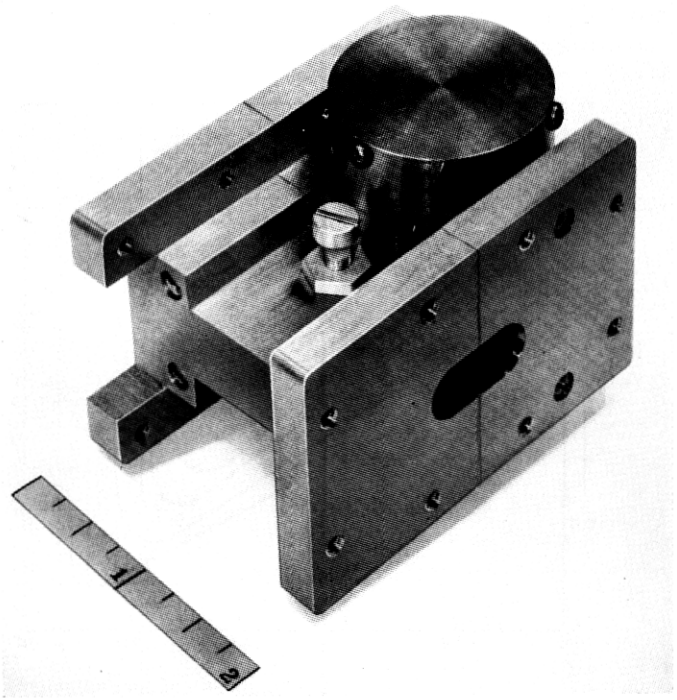

Fig. 3 — Ferrimagnetic limiter, showing the microwave cavity and external biasing magnet.

($\approx$0.3 oersteds) resulting in low thresholds (Fig. 2). Spherical geometry was chosen to minimize temperature effects since the ferromagnetic resonant frequency does not depend on the saturation magnetization, which varies with temperature.

II. ELECTRICAL DESIGN CONSIDERATIONS

2.1 *Insertion Loss and Limiting Threshold*

The transmission microwave cavity was made of reduced-height waveguide coupled to the external transmission lines with inductive irises. The cavity was excited in the TE_{101} mode as shown in Fig. 4. The YIG sphere was placed near the sidewall of the cavity and biased as shown. It is necessary to have a large ratio of sample to cavity volume so that the losses in the sample will represent a large change in the total cavity losses above the threshold (see Section 2.2). In this model it was found necessary to use spheres nominally 0.250 inch in diameter with cavities only slightly greater in height. Because of this large volume the sample contributes significant loss and reactance to the cavity mode below the threshold. The reactance contributed by a ferrimagnetic sample biased below the uniform precession resonance raises the cavity resonant frequency and thus can be compensated in part by a tuning screw placed in the maximum of the electric field, which will lower the cavity resonance by adding shunt capacitance. The transmission coefficient of the cavity at resonance is given by

$$T = \frac{1}{\left[1 + \frac{Q_e}{2Q_o}\right]^2} \tag{1}$$

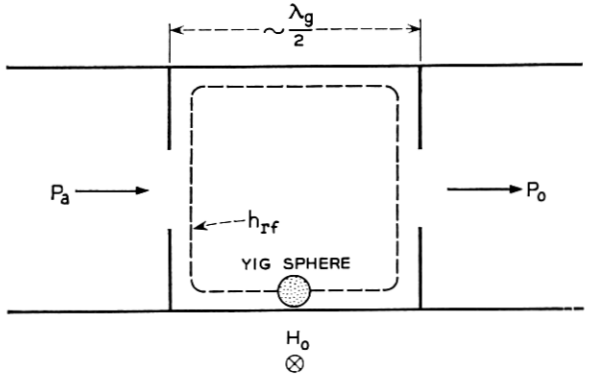

Fig. 4 — Schematic of the Telstar limiter.

where the loaded cavity $Q(Q_L)$ is given in terms of the external and unloaded Q's (Q_e and Q_o) by

$$\frac{1}{Q_L} = \frac{1}{Q_o} + \frac{2}{Q_e}.$$

In order to keep the low-level loss as low as possible, all precautions were taken to insure the largest value possible for Q_o. This included silver plating the cavity walls. (See Section III.) Thus the only electrical parameter available to maintain a low insertion loss is Q_e. However, the limiting threshold power also depends on Q_e as given by

$$P_{o\,\mathrm{crit}} = \frac{\omega}{Q_e} \frac{\mu_o h_{\mathrm{crit}}}{2} \int_{V_c} h^2 dV$$

where V_c is the cavity volume, with the sample placed where the RF magnetic field is maximum. Since the range of values of h_{crit}, at a given frequency, is bounded (Fig. 2) the specification of insertion loss and $P_{o\,\mathrm{crit}}$ are not independent. However, it was found possible to achieve a satisfactory insertion loss and still meet the threshold requirement given in Table I as well as the required Q (200) to serve the required filter function. The dc magnetic field required for this threshold was 1200 oersteds, resulting in $(\omega_o/\omega) = 0.840$ (neglecting the effect of crystalline anisotropy, as will be discussed presently). This operating point was chosen to lie somewhat on the low-field side of the minimum of the h_{crit} curve. The similar high-field point was found to have unsatisfactory temperature characteristics as well as a poorly defined break at threshold.

2.2 *Limiting Slope*

The behavior of the limiter in the nonlinear region of its operation depends critically on the ratio of sample to cavity volume. With the same cavity, reducing the sample size from 0.250 inch to 0.180 inch resulted in severe degradation of the limiting action. It was found that the limiting curve above the threshold was nearly a straight line over at least a 28-db dynamic range with a slope which decreased rapidly with sample volume. The sharpness of the discontinuity in the limiting curve from the linear to the nonlinear region was found to depend critically on the degree of sample polish. This result is unexplained on the basis of Suhl's theory. Experimental limiting curves are discussed in Section IV.

2.3 *Temperature Compensation*

Two limiter properties were found to vary to a significant degree over the temperature range given in Table I. These are the limiting threshold

and a thermal detuning resulting in increased low-level insertion loss. The variation in limiting threshold is due primarily to changes in h_{crit} caused by the temperature variation of the saturation magnetization ($4\pi M_s$), spin wave linewidth (ΔH_k), and anisotropy field (H_a). In the present case the crystal has cubic symmetry with the "easy" and "hard" magnetic axes long [111] and [100] directions, respectively. The temperature variations of $4\pi M_s$ and ΔH_k are such as to partially compensate the change in h_{crit} with respect to temperature, with the largest contribution being that due to variations in $4\pi M_s$; the net result is that h_{crit} increases with temperature. The anisotropy field can be used to compensate the residual temperature sensitivity, as can be shown using the curve in Fig. 5. This curve shows the variation in the effective bias magnetic field, including anisotropy, with respect to an angle θ measured from [100] as the sample is rotated about a [110] axis. In the two extreme cases $\theta = 0°, 54° 44'$, i.e., when the sample is oriented so that a "hard" and an "easy" axis are lined up along H_o, the effective field is given by

$$H_e\Big|_{[100]} = H_o - 2\frac{|K_1|}{M_s}$$
$$H_e\Big|_{[111]} = H_o + \frac{4}{3}\frac{|K_1|}{M_s} \qquad (2)$$

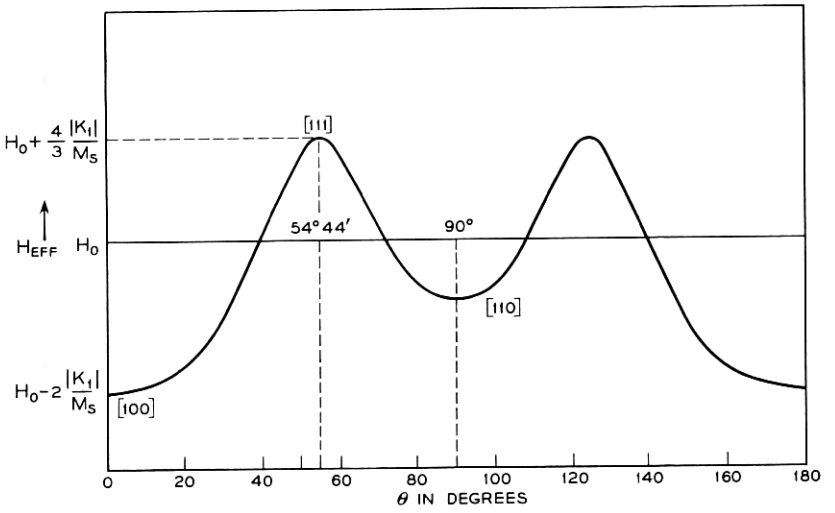

Fig. 5 — Effective static magnetic field, including anisotropy, for a cubic ferrimagnet for rotation about the [110] axis with $\theta = 0°$, corresponding to [100].

where K_1, the first-order anisotropy constant, is negative for YIG and decreases with temperature. The temperature variation of h_{crit} due to the temperature variation of H_e is given by

$$\frac{1}{h_{\text{crit}}}\frac{dh_{\text{crit}}}{dT} = \frac{1}{h_{\text{crit}}}\frac{\partial h_{\text{crit}}}{\partial H_e}\frac{dH_e}{dT}$$

where we see from Fig. 2 that $(\partial h_{\text{crit}}/\partial H_e) < 0$. Since it is necessary to compensate a positive value of $(1/h_c)(\partial h_c/\partial T)$ arising from changes in ΔH_k and $4\pi M_s$, it is seen that a positive value for dH_e/dT is needed, which can be obtained by orienting the sample with the dc magnetic field along [100]. Experimental results were obtained with orientation along both [100] and [111] which gave striking confirmation of the temperature compensation obtainable with this technique. The experimental results of Section IV show the effect of proper temperature compensation.

II. MECHANICAL DESIGN CONSIDERATIONS

13.1 *Cavity*

The limiter is constructed in a reduced-height, silver-plated magnesium cavity. The cavity is composed of two waveguide half-sections joined along the broad dimension, as shown in Fig. 3. Each half-section is of unit construction; the iris half-plates and the waveguide flanges at each end are an integral part of the machined piece to eliminate lowered Q's resulting from soldered iris plates. The over-all length of the cavity is 1.976 inches. The iris plates are 0.062 inch thick with centrally placed coupling irises (0.375 × 0.800 inch). Internal cross-section dimensions of the cavity are 0.400 inch high by 1.872 inches wide. The YIG sphere is placed 0.062 inch from the side wall of the cavity in a region of maximum RF magnetic field. The reduced-height cavity serves not only to give a large filling factor but to reduce appreciably the size and weight of the magnet required to bias the YIG sphere across the narrow waveguide dimension.

A silver-plated brass tuning screw is inserted in the broad dimension of the cavity and centrally placed along the length.

3.2 *Permanent Magnet*

An efficient permanent magnet capable of producing a field of approximately 1200 gauss across a 0.400-inch air gap was required in order to realize a practical limiter design. The magnet, designed for this application by M. S. Glass, contains two truncated cones of Alnico VI material of the proper length-to-diameter ratio to eliminate irreversible losses over the temperature range of interest. In addition it provides a very nearly

temperature-independent bias field. Two soft iron pole-pieces are used to concentrate the magnetic flux, and an outer case of heat treated tubing is used both as a return path and as an effective magnetic shield. The weight of the magnet assembly is approximately 9 ounces; the total weight of the limiter is 13 ounces.

3.3 *The YIG Sphere*

The diameters of the single-crystal YIG spheres used in the flight and test models of the satellite limiter ranged from 0.2470 inch to 0.2988 inch. Each sphere exhibited a highly polished surface which reduced the low-level insertion loss, made the slope transition more abrupt at the threshold and decreased the limiting slope.

The single-crystal YIG sphere was positioned in the cavity so that one of its three hard axes of magnetization was aligned along the direction of the static magnetic field. The hard magnetic axes of the YIG sphere were determined by first finding the four easy axes by allowing the sample to rotate freely in a uniform dc magnetic field so as to align itself along each of the [111] axes. Then a [100] or hard axis is uniquely defined and can be located and marked. This procedure eliminates the need for X-ray orientation and is sufficiently accurate for the required temperature compensation as shown in Section IV. The YIG sphere was supported 0.062 inch away from the cavity sidewall by encasing it in a Tellon package which was held firmly to the waveguide wall by a screw.

IV. PERFORMANCE

4.1 *Temperature Testing*

Fig. 6 shows the electrical characteristics of the 4080-mc limiter as a function of temperature. As noted, the compensated temperature performance of the device over the range from 35°F to 120°F was due to the alignment of a hard axis of magnetization of the YIG sphere with the direction of the applied dc magnetic field. All of the properties of the limiter fell within the specifications given in Table I over this temperature range.

4.2 *Mechanical Tests*

The limiter was subjected to the standard shock and vibration test with the following maximum test parameters:

Force	33 g
Frequency	40–2000 cps
Period	4.75 minutes

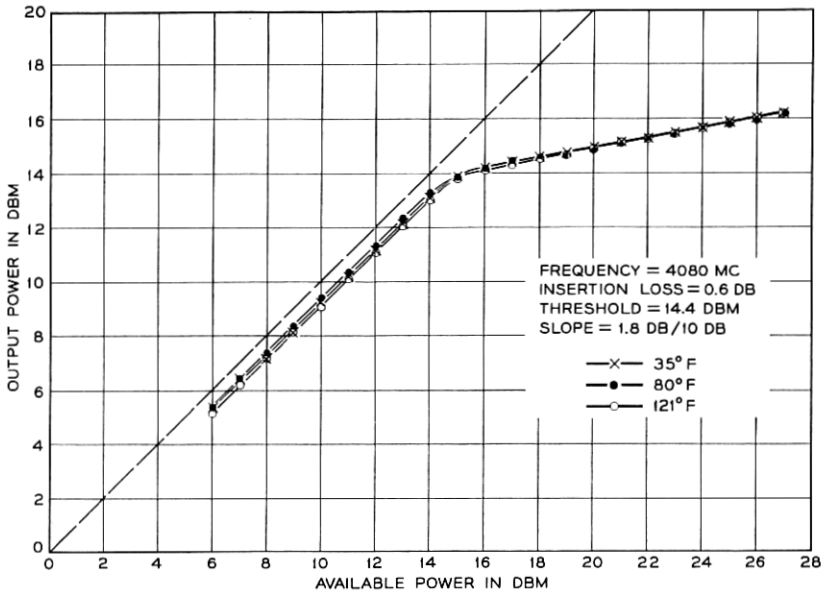

Fig. 6 — Experimental limiting curves for three operating temperatures. The YIG sample is oriented with a hard magnetic axis along the bias direction.

No degradation in the electrical performance of the limiter was observed following these tests. A centrifuge test was also performed with a maximum force of 30 g for three minutes and again no change in limiter performance was observed.

4.3 *Radiation Testing*

The ionizing radiation in the lower Van Allen belt consists of protons, electrons and gamma rays. The electrons have a moderate energy level (1 Kev to 100 Kev) and nearly all of them are stopped in the outer shell of the Telstar satellite. Nevertheless, electron radiation testing was conducted on the limiter, which is part of the electronic package within the satellite. Proton radiation testing was also performed on the limiter, since the protons of the lower Van Allen belt have relatively high energy (0.1 Mev to 1 Mev) and penetrate the entire satellite.

The irradiation test program on the limiter consisted of subjecting the single-crystal sphere of YIG and the Tellon package to the various types of radiation. Electrical tests were performed on a test limiter before and after radiation exposure, and it was found that the electron bombardment experiments had the largest effect. However, the electron energy

(1 Mev) corresponded to *unshielded* exposure in the lower Van Allen belt, and thus the effects under shielded conditions are expected to be much less than observed in this experiment. This effect probably is completely ascribable to electron radiation-induced dissipation in the Tellon holder. In the case of proton radiation with 10-Mev energy, slight degradation in the limiting slope characteristic was noted. It is conceivable that this also is attributable to the Tellon package; however, the highly polished YIG surface was observed to be slightly clouded. It is known that surface polish may have similar effects, and thus it is possible that there was an effect on the YIG sample primarily through surface damage. The gamma radiation test consisted of exposing the operating limiter to a low-intensity cobalt 60 source (1.3 curie) simulating conditions in the lower Van Allen belt. No effects on limiter characteristics were observed during the test.

V. CONCLUSIONS

As with many contributions to the Telstar project, the limiter development required considerable extension of existing device capabilities. Although the principle of ferrimagnetic limiting had been known for some time, there existed no well developed device technology or detailed design theory. The temperature stability requirements presented a particularly challenging problem. The basic understanding of ferromagnetic resonance and spin wave instability, particularly in single crystals, provided the basis for the rapid development of a design theory and limiter realization. The temperature dependence of the magnetocrystalline anisotropy (anisotropy field) provided the key which made possible the limiter design described in this paper.

VI. ACKNOWLEDGMENTS

The authors wish to acknowledge the many stimulating discussions with and contributions of R. C. LeCraw, E. G. Spencer, F. C. Rossol, V. Czarniewski, T. W. Mohr and J. Degan.

REFERENCES

1. Bodmer, M. G., Laico, J. P., Olsen, E. G., and Ross, A. T., The Satellite Traveling-Wave Tube, B.S.T.J., this issue, p. 1703.
2. Davis, C. G., Hutchinson, P. T., Witt, F. J., and Maunsell, H. I., The Spacecraft Communications Repeater, B.S.T.J., this issue, p. 831.
3. Suhl, H., Theory of Ferromagnetic Resonance at High Signal Powers J. Phys., and Chem. of Solids, **1**, April, 1957, pp. 209–227.